

A new phase of coesite SiO₂

A. Kirfe, G. Will

Mineralogisches Institut der Universität Bonn, Lehrstuhl für Mineralogie und Kristallographie,
Poppelsdorfer Schloss, D-5300 Bonn, Federal Republic of Germany

and J. Arndt

Mineralogisches Institut der Universität Tübingen,
Wilhelmstr. 56, D-7400 Tübingen Federal Republic of Germany

Received: February 22, 1979

Abstract. A coesite crystal synthesized from aqueous solution (Arndt and Rombach, 1976) under static high-pressure high-temperature conditions of 44–49 kb and 610°C was investigated by X-ray diffraction. From the lattice constants $a = 7.148(2) \text{ \AA}$, $b = 12.334(3) \text{ \AA}$, $c = 7.112(2) \text{ \AA}$, $\beta = 120.30(2)^\circ$, and the space group $P2_1/a$ we conclude the existence of another coesite phase, which is about 1% denser than the known phase with $C2/c$ (Gibbs et al., 1977). The overall arrangement of the atoms in the new phase is closely related to the $C2/c$ phase, but the SiO₄ tetrahedra are of considerably different sizes. The finding of a new, denser coesite phase implies that the silica phase diagram may consist of even more phases than presently known. The range of bond lengths and bond angles was used to check for linear correlations which would give supporting experimental evidence for the π -bond model in the silicate ion (Cruickshank, 1961).

Introduction

The silica high-pressure polymorph coesite was previously generally considered as a characteristic indicator of meteorite impact. However, Smyth and Hatton (1977) recently described coesite as a primary phase in a mantle-derived kyanite eclogite from the Roberts Victor kimberlite pipe, South Africa. This specimen therefore provided evidence that free silica exists in the upper mantle and that coesite may be a constituent of mantle eclogites located in regions within its stability field. The metastable preservation of primary coesite crystals thus supplies information about the pressure and temperature conditions at which the coesite-bearing rock equilibrated and about its cooling history when it was brought to the surface.

Table 1. Crystallographic data of SiO₂ (Coesite)

	This work	Gibbs, Prewitt, and Baldwin (1977)	Araki and Zoltai (1969)
<i>a</i> (Å)	7.148(2)	7.135(1)	7.173(4)
<i>b</i> (Å)	12.334(3)	12.372(1)	12.328(6)
<i>c</i> (Å)	7.112(2)	7.173(1)	7.175(4)
β (°)	120.30(2)	120.36(1)	120.00(4)
<i>V</i> (Å ³)	541.3(2)	546.4(3)	549.5
S.G.	<i>P</i> 2 ₁ / <i>a</i>	<i>C</i> 2/ <i>c</i>	<i>C</i> 2/ <i>c</i>
Conditions	44–49 Kb, 610°C	65 Kb, 110°C	
<i>Z</i>	16	16	16
ρ_x (g/cm ³)	2.948(1)	2.921(2)	2.904

The crystal structure of coesite was first determined by Zoltai and Buerger (1959), reinvestigated by Araki and Zoltai (1969), and recently once more studied in detail by Gibbs et al. (1977) (Table 1). The latter authors corroborated the space group *C*2/*c*, but reported for the first time a monoclinic angle deviating slightly from 120°. They studied intensively the correlations between Si–O bond lengths, bond angles in and between the SiO₄ tetrahedra, and bond populations. As a result they presented strong evidence for the validity of Cruickshank's (1961) assertion, that the bonding in the silicate ion involves overlaps of the 3d and 2p orbitals of Si and O, respectively. Under this assumption short Si–O bonds are expected to correlate with wide Si–O–Si angles and vice versa.

In the course of the upper mantle research activities Arndt and Rombach (1976) have synthesized coesite crystals under hydrothermal conditions. One of these crystals has been investigated by us in more detail by X-ray diffraction analysis and in the course of this study we have found a coesite phase of symmetry lower than *C*2/*c* (Gibbs et al., 1977). We wish to report the results of this refinement in this paper.

Experimental

Coesite crystals were synthesized from aqueous solutions at pressures ranging from about 35 to 50 kb and at temperatures between 430 and 700°C. Since the experimental synthesis procedures have been described in detail by Arndt and Rombach (1976), only a brief summary will be given here.

The experiments were made in a "belt" type high-pressure apparatus using leak-proof stainless steel containers for the aqueous solutions. In two runs gold liners were inserted into the steel containers. Quartz, silica gel, and silica glass were used as starting materials in charges containing between 67

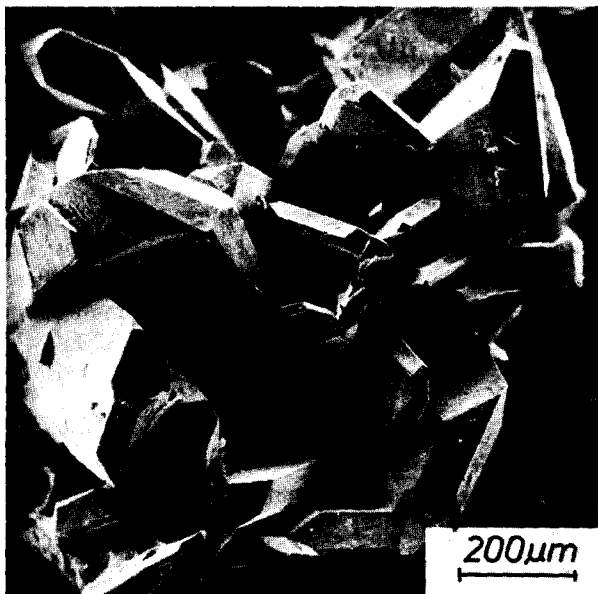


Fig. 1. Scanning electron microscope photograph of hydrothermally synthesized aggregate of lath-shaped coesite crystals. The presently investigated coesite crystal stems from this run. For run data see text

and 92 wt. % H₂O. In the various runs the charges were kept at constant P and T between 33 and 320 min and then cooled at various cooling rates to room temperature at approximately constant P. Detailed run data are given in Table 1 in the paper of Arndt and Rombach (1976).

The pressures given for the synthesis experiments are based on a calibration curve of ram load versus pressure fixed points. As was pointed out already by Arndt and Rombach (1976), the true pressures in the containers are very likely to be about 20% lower.

The crystal used for investigation in this study was synthesized in run No. 8 of Arndt and Rombach (1976) at the following experimental conditions:

Pressure: 44–49 kb; temperature: 610°C; time 150 min; cooling rate 8°C/min; 14 wt. % quartz as starting material. The synthesis products were aggregates of well developed lath-shaped coesite crystals (Fig. 1) with lengths up to 0.8 mm.

The specimen selected for the X-ray diffraction experiments had maximum dimensions of 0.1 × 0.35 × 0.35 mm. The preliminary study for the space group symmetry and the crystal quality was done by Weissenberg-film techniques. The photographs of the layers (*h0l*), (*h1l*), and (*h2l*) clearly

reveal violations of the space group symmetry $C2/c$ as determined by Gibbs et al. (1977). The observed conditions for the reflections were:

$$\begin{aligned} (0k0) \quad k &= 2n \\ (h0l) \quad h &= 2n \end{aligned}$$

leading to the space-group $P2_1/a-C_{2h}^5$.

Further studies of the crystal were done on a Syntex $P2_1$ computer-controlled four circle diffractometer. The lattice constants were refined by least-squares methods from the adjusted angular settings of 25 independent reflections. Table 1 shows the results and related crystallographic data in comparison with the values reported earlier by Gibbs, Prewitt, and Baldwin (1977) and by Araki and Zoltai (1969). All lattice constants are found to differ significantly from earlier publications. With $Z = 16$ and four SiO₂ in the asymmetric unit, the unit cell is about 1% smaller, yielding about a 1% higher calculated density of 2.948(1) g/cm³. Already these findings indicate that the structure of the phase must be different from the earlier reported atomic arrangement.

The complete data-collection was done using MoK α radiation ($\lambda = 0.71069$ Å), monochromatized by a graphite monochromator, in the ω -scan mode with a 2° scan range. The scan speed was between 1.0 and 10.0°/min, and the total background counting time equalled the time spent for the peak count. Six standard reflections were remeasured after every 28 records. For a maximum value of 70° in 2θ , 3124 reflections (including standards) were measured, resulting in a set of 2327 unique reflections, of which 937 were regarded as unobserved [$I < 3\sigma(I)$].

The intensities were corrected for the fluctuations of the sums of the intensities of the check-reflections. No absorption correction was applied in which 937 were regarded as unobserved [$I < 3\sigma(I)$].

The structure was solved with Multan (Germain, Main, and Woolfson, 1971) using $116|E_h|^s$ greater 1.5 and $1354\Sigma 2$ relationships. The phase set with the highest CFOM yielded an E-map clearly showing the positions of the 12 atoms of the asymmetric unit. Refinement was by full matrix-least-squares with a Cruickshank weighting scheme and anisotropic temperature factors. [$w = 46.9/(0.025|F|^2 - 2.50|F| + 100)$ for $F > 50.0$ and $w = 0.025|F|$ for $F \leq 50.0$]. Assuming predominantly covalent bonding, the scattering factors for neutral Si and O were taken from the Int. Tables of Crystallography IV, 1974. An isotropic extinction factor g (Zachariasen, 1963) was included in the list of variables (final value $g = 3 \times 10^{-5}$). With 19 reflections excluded from refinement due to either extinction or poor counting statistics the final R was 0.096 (0.047 omitting unobserveds) and $R_w = 0.038$ (0.036). The goodness of fit was 0.89. A list of the observed and calculated structure factor tables can be obtained through the authors.

Table 2. Atomic fractional coordinates ($\times 10^4$) with e.s.d's in parentheses

Atom	<i>x</i>	<i>y</i>	<i>z</i>	Atom	<i>x</i>	<i>y</i>	<i>z</i>
Si(1)	3224(1)	3585(1)	3910(1)	O(3)	2351(3)	3548(2)	5609(3)
Si(2)	6864(1)	3582(1)	1106(1)	O(4)	5791(3)	3726(2)	5144(3)
Si(3)	7874(1)	4086(1)	7432(1)	O(5)	7865(3)	4648(1)	2681(3)
Si(4)	2190(1)	4074(1)	7562(1)	O(6)	2083(4)	4581(2)	2334(4)
O(1)	2498(17)	2515(3)	2486(20)	O(7)	4275(3)	3738(2)	−184(3)
O(2)	39(7)	3662(1)	7520(9)	O(8)	7700(4)	3530(2)	−597(4)

Table 3. Atomic thermal parameters U_{ij} [$\times 10^4 \text{ \AA}^2$] with e.s.d's in parentheses

Atom	U_{11}	U_{22}	U_{33}	U_{12}	U_{13}	U_{23}	B_{eq} [\AA^2]
Si(1)	66(3)	35(3)	70(3)	−9(2)	32(2)	−14(2)	0.63
Si(2)	49(3)	16(3)	66(3)	−1(2)	40(2)	9(2)	0.58
Si(3)	96(6)	42(5)	105(6)	4(4)	79(5)	6(6)	1.09
Si(4)	27(5)	14(5)	39(5)	4(4)	64(4)	1(5)	0.32
O(1)	131(7)	30(5)	108(7)	−15(5)	63(6)	−28(5)	1.00
O(2)	66(6)	69(6)	124(6)	−25(15)	61(5)	−23(18)	0.88
O(3)	116(8)	115(8)	63(8)	−16(7)	58(7)	−53(7)	0.94
O(4)	67(8)	90(8)	127(9)	−24(6)	58(7)	−45(7)	0.92
O(5)	96(8)	20(8)	82(8)	0(6)	52(7)	−11(6)	0.82
O(6)	164(10)	26(8)	155(10)	15(7)	63(8)	0(7)	1.46
O(7)	66(8)	114(8)	92(2)	0(6)	14(6)	26(7)	0.99
O(8)	188(10)	77(8)	179(10)	16(8)	153(9)	10(8)	2.03

Results

The positional and anisotropic thermal parameters U_{ij} of the atoms are given in Tables 2 and 3. The equivalent isotropic temperature factors B_{eq} calculated from

$$B_{\text{eq}} = \frac{4}{3} \sum_i \sum_j \beta_{ij} a_i a_j$$

are included in Table 3. The expression for the temperature factor is $\exp(\beta_{11}h^2 + \beta_{22}k^2 + \beta_{33}l^2 + 2\beta_{12}hk + 2\beta_{13}hl + 2\beta_{23}kl)$ and $U_{ij} = \beta_{ij}/2\pi^2 a_i a_j$. The arrangement of the atoms is very similar to that of the structure as reported by Gibbs et al. (1977), but it is significantly distorted from $C2/c$ symmetry. The relationship between the two structures can be deduced from Fig. 2 showing projections along [010] of corresponding SiO₄-tetrahedra (one asymmetric unit of $P2_1/a$, two units of $C2/c$).

The new phase of lower symmetry can be obtained approximately from the old phase of $C2/c$ by a rotation of 60° around [010] and a subsequent

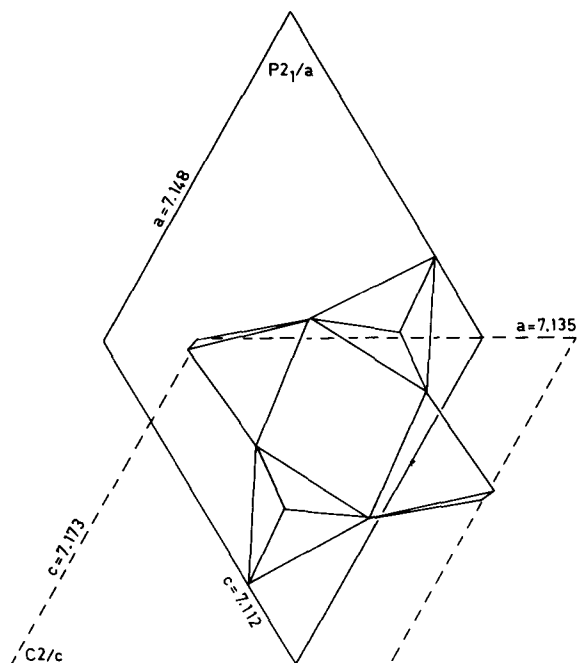


Fig. 2. Relationship between coesite phases *C2/c* and *P2₁/a*. Projection of SiO₄-tetrahedra (asymmetric unit in *P2₁/a*, two asymmetric units in *C2/c*) and unit cells along [010]. The origin of the *C2/c* unit cell is in $\frac{1}{4}, \frac{1}{4}, \frac{1}{4}$ with respect to *P2₁/a*

translation along [111] by $(\frac{1}{4}, \frac{1}{4}, \frac{1}{4})$. Thus the approximate transformation of atomic coordinates is given by:

$$\begin{pmatrix} x' \\ y' \\ z' \end{pmatrix} \approx_{P2_1/a} \begin{pmatrix} 1 & 0 & -1 \\ 0 & 1 & 0 \\ 1 & 0 & 0 \end{pmatrix} \begin{pmatrix} x \\ y \\ z \end{pmatrix} +_{C2/c} \begin{pmatrix} 0.25 \\ 0.25 \\ 0.25 \end{pmatrix}$$

A comparison of the calculated transformed coordinates with the final refined positional parameters shows that the Si frameworks of both structures are almost congruent. The symmetry of the investigated crystal is lowered mainly because of differences in the oxygen arrangement. As a consequence the asymmetric unit consists of four different SiO₄-tetrahedra leading to 16 nonequivalent Si–O bonds and 36 nonequivalent O–Si–O valence angles. The values are summarized in Tables 4 and 5. Inspection of these tables clearly reveals the different sizes and different degrees of distortion of the units. The adjacent Si(1)- and Si(4)-tetrahedra, sharing the O(3) atom, have mean Si–O bond lengths of 1.594 Å and are fairly regular with valence angles differing not more than 1.8° from the ideal tetrahedral

Table 4. Distances Si–O [Å] and angles O–Si–O [°] with e.s.d.'s in parentheses

Si(1)–O(1)	1.583(6)	O(1)–Si(1)–O(6)	108.0(3)
Si(1)–O(6)	1.584(2)	O(1)–Si(1)–O(4)	110.9(4)
Si(1)–O(4)	1.594(2)	O(1)–Si(1)–O(3)	109.2(3)
Si(1)–O(3)	1.616(1)	O(6)–Si(1)–O(4)	110.1(1)
		O(6)–Si(1)–O(3)	107.2(1)
	<1.594>	O(4)–Si(1)–O(3)	111.3(1)
			<109.45>
Si(2)–O(1)	1.597(6)	O(1)–Si(2)–O(8)	109.5(3)
Si(2)–O(8)	1.599(2)	O(1)–Si(2)–O(7)	109.9(4)
Si(2)–O(7)	1.610(2)	O(1)–Si(2)–O(5)	111.6(3)
Si(2)–O(5)	1.640(2)	O(8)–Si(2)–O(7)	109.5(1)
		O(8)–Si(2)–O(5)	110.4(1)
	<1.611>	O(7)–Si(2)–O(5)	105.9(1)
			<109.46>
Si(3)–O(2)	1.604(2)	O(2)–Si(3)–O(4)	109.2(2)
Si(3)–O(4)	1.618(2)	O(2)–Si(3)–O(8)	108.7(1)
Si(3)–O(8)	1.621(2)	O(2)–Si(3)–O(6)	110.7(1)
Si(3)–O(6)	1.650(2)	O(4)–Si(3)–O(8)	108.7(1)
		O(4)–Si(3)–O(6)	109.6(1)
	<1.623>	O(8)–Si(3)–O(6)	109.9(1)
			<109.47>
Si(4)–O(5)	1.584(2)	O(5)–Si(4)–O(3)	108.6(1)
Si(4)–O(3)	1.589(1)	O(5)–Si(4)–O(7)	109.1(1)
Si(4)–O(7)	1.597(2)	O(5)–Si(4)–O(2)	110.0(1)
Si(4)–O(2)	1.606(4)	O(3)–Si(4)–O(7)	109.2(1)
		O(3)–Si(4)–O(2)	110.2(1)
	<1.594>	O(7)–Si(4)–O(2)	109.7(2)
			<109.47>

Si–O = 1.6055

angle. The regularity and similarity of these tetrahedra is also reflected in the mean O–O distances of 2.602 Å and 2.604 Å, respectively. The other two SiO₄ tetrahedra with Si(2) and Si(3) are significantly larger with mean Si–O bond lengths of 1.611 Å and 1.623 Å, and mean O–O distances of 2.630 Å and 2.640 Å, respectively. In addition, the Si(2) tetrahedron with an O(7)–Si(2)–O(5) angle of 105.9° is much more distorted than the others. The average of all Si–O bonds yields 1.6055 Å, which compares well with the mean bond length of 1.6069 Å found in the *C2/c* phase. The overall O–O distance is 2.6190 Å, and the mean Si–Si distance 3.0686 Å compared to 2.6293 Å and 3.0870 Å taken from Gibbs et al. (1977). These values exhibit significant differences and their ratio of 0.996 and 0.994, respectively

Table 5. Distances O–O [Å], Si–Si [Å] and angles Si–O–Si (°) with e.s.d.'s in parentheses

O(1)–O(6)	2.564(5)	Si(1)–Si(2)	3.180(1)
O(1)–O(3)	2.608(7)	Si(3)–Si(4)	3.040(1)
O(1)–O(4)	2.617(9)	Si(1)–Si(4)	3.097(1)
O(3)–O(6)	2.577(2)	Si(1)–Si(3)	3.050(1)
O(3)–O(4)	2.650(3)	Si(2)–Si(4)	3.011(1)
O(4)–O(6)	2.605(3)	Si(1)–Si(3)	3.003(1)
		Si(2)–Si(4)	3.064(1)
	<2.604>	Si(2)–Si(3)	3.104(1)
O(1)–O(8)	2.608(7)		
O(1)–O(7)	2.625(9)		<3.0686>
O(1)–O(5)	2.676(4)	Si(1)–O(1)–Si(2)	177.8(7)
O(5)–O(7)	2.591(3)	Si(3)–O(2)–Si(4)	142.5(1)
O(5)–O(8)	2.659(2)	Si(1)–O(3)–Si(4)	150.2(2)
O(7)–O(8)	2.620(3)	Si(1)–O(4)–Si(3)	143.4(1)
		Si(4)–O(5)–Si(2)	138.2(1)
	<2.630>	Si(1)–O(6)–Si(3)	136.4(1)
O(2)–O(8)	2.623(4)	Si(2)–O(7)–Si(4)	145.7(1)
O(2)–O(4)	2.628(5)	Si(2)–O(8)–Si(3)	149.2(2)
O(2)–O(6)	2.677(4)		
O(4)–O(6)	2.605(3)	Selected angles O–O–O	
O(4)–O(8)	2.633(2)	O(6)–O(1)–O(5)	178.6(4)
O(6)–O(8)	2.678(3)	O(8)–O(1)–O(3)	179.2(4)
		O(4)–O(1)–O(7)	178.4(4)
	<2.640>	O(4)–O(2)–O(7)	176.1(1)
O(2)–O(5)	2.612(3)	O(3)–O(2)–O(8)	173.4(1)
O(2)–O(7)	2.618(5)		
O(2)–O(3)	2.620(4)		
O(3)–O(5)	2.577(3)		
O(3)–O(7)	2.596(2)		
O(5)–O(7)	2.591(3)		
	<2.602>		

O–O = 2.6190

corresponds to the ratio of calculated densities (0.991). The small but significantly higher density in $P2_1/a$ as compared to $C2/c$ is thus reflected in the closer oxygen packing in average as well as in the shorter Si–O distances.

The question arises whether there is a correlation between bond distances and angles. This was studied by plotting scatter diagrams depicted in Figures 3 and 4. Figure 3 shows the Si–O bond lengths versus the mean value $\langle O-Si-O \rangle_3$ of the valence angles, in which the considered bond is involved. A linear regression analysis yielded a correlation coefficient of only $r = 0.0566$. Though the range of bond lengths and angles is large enough there is no significant correlation between $d(Si-O)$ and $\langle O-Si-O \rangle_3$. This is in contrast to the prediction of EHMO-theory and to the finding of Gibbs et al.

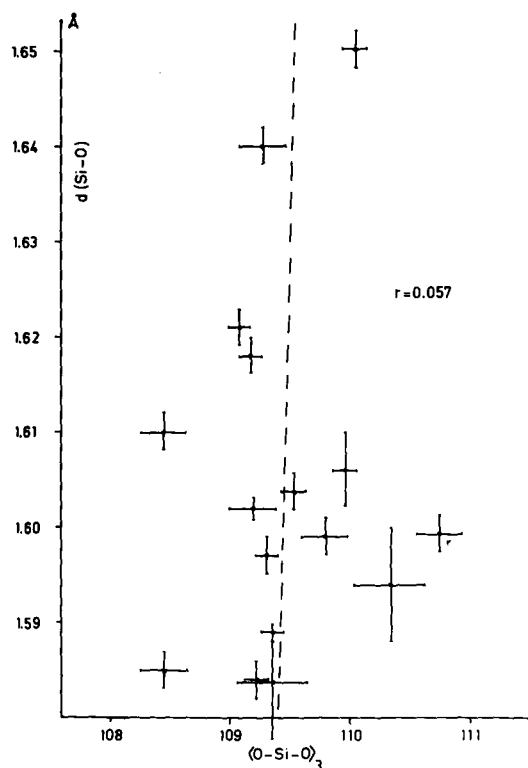


Fig. 3. Scatter diagram of $d(\text{Si}-\text{O})$ versus $\langle \text{O}-\text{Si}-\text{O} \rangle_3$, the mean O-Si-O angle common to the Si-O bond

(1977), who reported a $r = 0.761$. The second diagram (Fig. 4) shows the average $d(\text{Si}-\text{O})$ distances of bonds involved in Si-O-Si angles versus the negative reciprocal cosines of these angles. In this case the linear regression analysis shows a linear dependency according to:

$$\bar{d}(\text{Si}-\text{O}) = 0.0607 \cdot \chi(\text{Si}-\text{O}-\text{Si}) + 1.5317$$

and a correlation coefficient of $r = 0.90$. This result agrees well with the corresponding value of the $C2/c$ phase with $r = 0.98$ and a slope of approximately 0.069. In agreement with Gibbs et al. we can reject at a 0.001 level the hypothesis that $\bar{d}(\text{Si}-\text{O})$ is not dependent on $\chi(\text{Si}-\text{O}-\text{Si})$.

A survey of the temperature factors shows that the thermal vibrations are generally somewhat larger than those reported for the $C2/c$ phase. The mean $\bar{B}(\text{Si}) = 0.65 \text{ \AA}^2$ and $\bar{B}(\text{O}) = 1.13 \text{ \AA}^2$ exceed the corresponding values of the $C2/c$ phase by 29% and 25%, respectively. This may be due to imperfections in the crystal resulting from the cooling history, to a lesser extent also to a

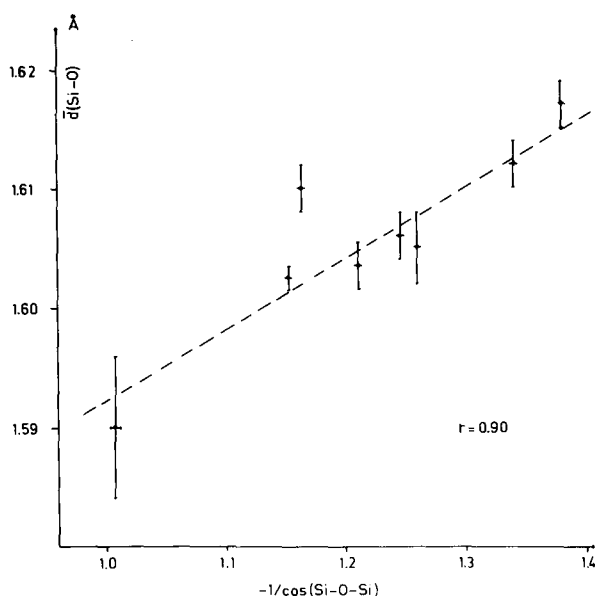


Fig. 4. Scatter diagrams of $\bar{d}(\text{Si-O})$, the mean Si-O distance in the Si-O-Si angle, versus $-1/\cos(\text{Si-O-Si})$. From the linear regression analysis with $r = 0.90$ the hypothesis that $\bar{d}(\text{Si-O})$ might not be dependent on $1/\cos(\text{Si-O-Si})$ can be rejected at the 0.001 level

systematic error in the data. More surprising is the range of the isotropic temperature factors. For the Si atoms they range from 0.32 \AA^2 to 1.09 \AA^2 , and for the O atoms from 0.82 \AA^2 to 2.03 \AA^2 . If we are in doubt about the individual temperature results, which may be falsified for unknown reasons, we can check them in a statistical way. Assuming every SiO₄ tetrahedron as a rigid body with isotropic vibrational behavior, one can assign to each of them the average of the involved atomic temperature factors yielding $\bar{B}(\text{Si1}) = 0.99 \text{ \AA}^2$, $\bar{B}(\text{Si2}) = 1.08 \text{ \AA}^2$, $\bar{B}(\text{Si3}) = 1.45 \text{ \AA}^2$, and $\bar{B}(\text{Si4}) = 0.79 \text{ \AA}^2$. These values correlate linearly with the sizes of the tetrahedra, expressed by the mean Si-O or O-O bond distances (Tables 4 and 5) with a correlation coefficient $r = 0.92$. This is evidence for the principal correctness of the refined temperature factors, which reflect that the different tightly bound SiO₄ tetrahedra allow different vibrational displacements of their constituting atoms. Figure 5 shows an ORTEP-drawing (Johnson, 1965) of the asymmetric unit viewed along the *b*-axis, which also gives an impression of the different thermal vibrations of the atoms.

Conclusions

The investigation of the crystal structure of a new coesite crystal shows unambiguously that this crystal belongs to a high pressure SiO₂-phase of

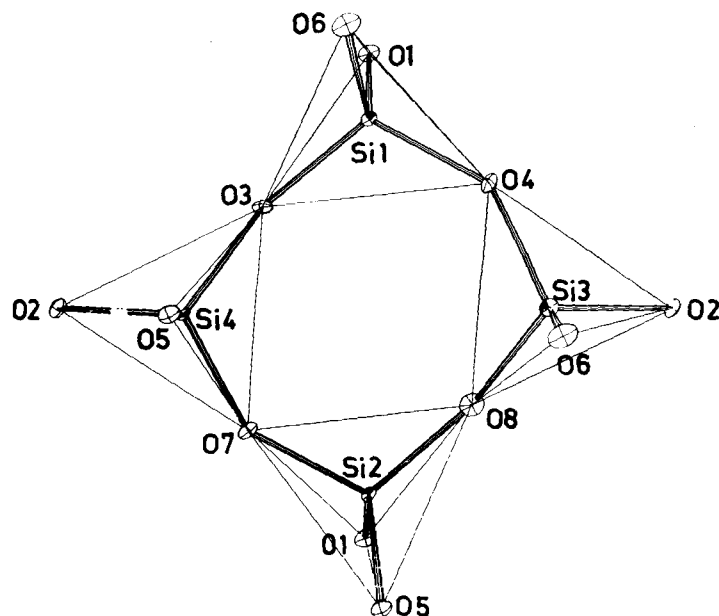


Fig.5. ORTEP drawing of the asymmetric unit in coesite ($P2_1/a$)

lower symmetry than $C2/c$ and of higher density than all earlier reported phases (Araki and Zoltai, 1969; Sclar et al., 1962; Dacheille and Roy, 1959; Ramsdell, 1955). There is a close structural relationship between the two phases, which can be described approximately by a simple transformation scheme. The increase of density is achieved by a distortion of the arrangement of SiO₄ tetrahedra and by an averaged shortening of the interatomic bond distances, although some individual Si–O and O–O bonds are found to be significantly longer than in the $C2/c$ phase. This applies especially for one (Si3) of the four nonequivalent SiO₄ tetrahedra.

The resulting relatively wide range of bond lengths and bond angles provides useful material for testing correlations which can support the Cruickshank π -bond model in the silicate ion. This is the case for the $\bar{d}(\text{Si}-\text{O})$ vs $-1/\cos(\text{Si}-\text{O}-\text{Si})$ relation; however, no significant indication could be found that $\bar{d}(\text{Si}-\text{O})$ is linearly dependent on $\langle \text{O}-\text{Si}-\text{O} \rangle_3$.

What conclusions can be drawn with respect to the SiO₂ phase diagram? Considering these new results and taking into account various preceding reports on coesite, it seems that "coesite" describes more than a unique phase of SiO₂. The two coesite phases can be distinguished also on powder diffraction diagrams due to clear differences in the extinction condition. We can assert conclusively that with increasing pressure there may exist even denser phases of coesite before the distinctive phase transformation into

stishovite takes place. Further syntheses of coesite stemming from higher pressure ranges and thorough structural investigations are therefore desirable.

References

- Araki, T., Zoltai, T.: Refinement of a coesite structure. *Z. Kristallogr.* **129**, 381–387 (1969)
- Arndt, J., Rombach, N.: Synthesis of coesite from aqueous solutions. *J. Crystal Growth* **35**, 28–32 (1976)
- Cruikshank, D. W. J.: The role of 3 d-orbitals in π -bonds between (a) silicon, phosphorus, sulfur, or chlorine and (b) oxygen or nitrogen. *J. Chem. Soc.* 5486–5504 (1961)
- Dachille, F., Roy, R.: High pressure region of the silica isotypes. *Z. Kristallogr.* **111**, 451–461 (1959)
- Germain, G., Main, P., Woolfson, M. M.: The application of phase relationships to complex structures. *Acta Crystallogr. A* **27**, 368–376 (1971)
- Gibbs, G. V., Prewitt, C. T., Baldwin, K. J.: A study of the structural chemistry of coesite. *Z. Kristallogr.* **145**, 108–123 (1977)
- Johnson, C. K.: ORTEP, a FORTRAN thermal ellipsoid plot program for crystal structure illustrations. U.S. Atomic Energy Commission Rep. ORNL-3794 (1965)
- Ramsdell, L. S.: The crystallography of "Coesite". *Amer. Mineral.* **40**, 975–982 (1955)
- Sclar, C. B., Carrison, L. C., Schwartz, C. M.: Optical crystallography of coesite. *Amer. Mineral.* **47**, 1292–1302 (1962)
- Smyth, J. R., Hatton, C. J.: A coesite-sanidine grosspydite from the Roberts Victor kimberlite. *Earth Planet. Sci. Lett.* **34**, 284–290 (1977)
- Zachariasen, W. H.: The secondary extinction correction. *Acta Crystallogr.* **16**, 1139–1144 (1963)
- Zoltai, T., Buerger, M. J.: The crystal structure of coesite, the dense, high-pressure form of silica. *Z. Kristallogr.* **111**, 129–141 (1959)